Journal of Thermal Analysis and Calorimetry, Vol. 55 (1999) 681-690

TG MEASUREMENTS OF THE OXIDATION KINETICS OF Fe–Cr ALLOY WITH REGARD TO ITS APPLICATION AS A SEPARATOR IN SOFC

T. Brylewski[1*], *T. Maruyama*[1], *M. Nanko*[1] *and K. Przybylski*[2]

[1]Department of Metallurgical Engineering, Faculty of Engineering, Tokyo Institute of Technology (TIT), 2-12-1 O-okayama, Meguro-ku, Tokyo 152, Japan
[2]Department of Solid-State Chemistry, Faculty of Materials Science and Ceramics, University of Mining and Metallurgy (AGH), al. Mickiewicza 30, 30-059 Cracow, Poland

Abstract

The high-temperature oxidation behavior of a ferritic alloy (SUS 430) in a SOFC environment, corresponding to the anode (H_2/H_2O gas mixture) and cathode (air) operating conditions, was determined with regard to application of the alloy as a metallic separator material in SOFC. The oxidation kinetics of Fe–16Cr alloy (SUS 430), was studied by thermogravimetry in H_2/H_2O gas mixtures with p_{H_2}/p_{H_2O}=94/6 and 97/3 and in air, in the temperature range 1023–1223 K, for 3.6 up to 1080 ks. It was found that the protective oxide scale, composed mainly of Cr_2O_3 with uniform thickness and excellent adhesion to the metal substrate, grows in accordance with the parabolic rate law. The dependence of the parabolic rate constant, k_p, of the scale on temperature obeys the Arrhenius equation: $k_p=6.8\times10^{-4}$ exp (–202.3 kJ $mol^{-1}R^{-1}T^{-1}$) for H_2/H_2O gas mixtures with p_{H_2}/p_{H_2O}=94/6. The determined k_p was independent of the oxygen partial pressure in the range from 5.2×10^{-22} to 0.21 atm at 1073 K, which means that the rates of growth of the scale on Fe–16Cr alloy in the above-mentioned atmospheres are comparable. The oxidation test results on Fe–16Cr alloy in H_2/H_2O gas mixtures and air demonstrate the applicability of SUS 430 alloys as a separator for SOFC.

Keywords: chromia, Fe–Cr alloy, gas-solid reaction kinetics, H_2/H_2O gas mixtures, oxidation

Introduction

In recent years, the high-temperature solid oxide fuel cells (SOFC) have been extensively investigated as a new electric power generating system, since they have the potential of converting the chemical energy of the reactants directly into electrical energy with a high conversion efficiency [1]. Moreover, the advantages

* Present address: Department of Solid-State Chemistry, Faculty of Materials Science and Ceramics, University of Mining and Metallurgy (AGH), al. Mickiewicza 30, 30-059 Cracow, Poland

1418–2874/99/ $ 5.00

Akadémiai Kiadó, Budapest
Kluwer Academic Publishers, Dordrecht

of the SOFC are their environmental compatibility, modularity and siting flexibility [1]. The planar-type SOFC have been proposed for application in a modern automobile [1]. In the planar design of SOFC stacks, the individual cells, consisting of solid electrolyte (ZrO_2:Y_2O_3) sandwiched between an anode and a cathode, are interconnected by an electrical conductor, which simultaneously acts as a gas separator and a distributor in the anode and cathode gas counterflow [1]. Such specific conditions of separator exploitation determine the particular requirements of the materials to be used for its construction. The most important are: high oxidation resistance, high electrical conductivity, a thermal expansion coefficient close to that of an electrolyte material, high mechanical strength, gas-tightness and machinability.

The commonly used ceramic separators of $LaCrO_3$ doped with either SrO or CaO exhibit high electrical conductivity and high corrosion resistance in the SOFC environment, corresponding to the anode (H_2/H_2O gas mixtures) and cathode (air) operating conditions [1]. The disadvantages of such materials are their poor resistivity to sudden temperature changes, the permeability of H^+ and O^{2-} and difficulties in producing separators of complex shapes. The chromia-forming alloy may offer a potential alternative for ceramic separators [2]. Alloys are quietly dense not to permit gas leakage and display high oxidation resistance by forming Cr_2O_3 on their surface as a result of the selective oxidation of Cr. However, chromium oxide has poor electrical conductivity, which increases in proportion to its thickness during the oxidation process. Recent studies [2–4] have demonstrated that the electrical conductivity of Cr_2O_3 formed on the chromia-forming alloy can be improved by applying a conducting oxide layer of $(La,Sr)CoO_3$ as a coating on the surface of these alloys.

From among the many tested alloys, the ferritic alloys seem to be promising materials for the construction of separators of planar-type SOFC operating at 1073 K, on account of their following advantages in comparison with those of other Ni or Co-based alloys [5–7]. First, the thermal expansion coefficients of these alloys are close to those of solid electrolytes of stabilized zirconia (for ZrO_2:Y_2O_3, $\Delta\alpha=10\cdot10^{-6}$ [K^{-1}]; for Fe–Cr, $\Delta\alpha=9–12\cdot10^{-6}$ [K^{-1}]). Secondly, the iron-based scaling-resistant alloys have chemical stability due to the high oxidation resistance of the Cr_2O_3 formed with good adhesion on the Fe–Cr alloy at elevated temperature in air and oxygen, and also in H_2/H_2O and $H_2/H_2O/H_2S$ gas mixtures, and the cost of fabrication of these alloys is considerably lower than that of other Ni or Co-based alloys. An additional important advantage of Fe–16Cr alloy coated with a $La_{0.6}Sr_{0.4}CoO_3$ layer by spray-pyrolysis is the low electrical resistance in comparison with that of a commercially available ceramic separator made of $La_{0.85}Sr_{0.15}CrO_3$ [6, 7].

As noted above, an important requirement for a metallic separator material is that the electrical resistivity across the oxide scale is kept at a low level. In order to evaluate the predicted change with time in the electrical resistivity of the oxide

scale formed on the alloy, a knowledge of the scale thickness is necessary, which can be determined from the oxidation kinetics results. Moreover, the rate of oxidation the alloy can be applied to design a separator with appropriate geometric parameters, ensuring its long-time exploitation (≥10000 h) in the SOFC environment.

The objective of this work is a thermogravimetric experimental study of the kinetics of oxidation of Fe–16Cr (SUS 430) alloy under both H_2/H_2O gas mixture and air atmospheres.

Experimental

The material selected for the experiments was SUS 430 stainless steel (Nippon Steel Corp., Japan), the results of chemical analysis of which are listed in Table 1. This alloy was produced by the manufacturer using a standard industrial process called '2B', as described in [8]. No further treatment was performed on the surface, and the alloy was used as-received for the present study.

Table 1 Chemical composition of SUS 430 alloy

Element	Fe	Cr	Mn	Si	Ni	Al	C	P	S
Mass/ %	82.9	16.31	0.21	0.35	0.12	0.11	0.048	0.023	0.0006

The Fe–16 mass per cent Cr alloy coupons for the oxidation test were prepared by a standard metallographic procedure, including cutting in the form of rectangular plates with a thickness of 1.0–1.3 mm and an area of 10×10 mm (mass about 1 g); mechanical abrading on all faces with silicon carbide papers of increasing fineness (from 100 up to 2000-grit); polishing with diamond paste to a finish of 1.4 μm; and finally washing in an ultrasonic cleaner with distilled water and with acetone.

Oxidation experiments on the Fe–16Cr alloy were carried out under isothermal conditions in controlled H_2/H_2O gas mixtures with p_{H_2}/p_{H_2O}= values of 94/6 or 97/3, at 1073 K, and in a static air atmosphere in the temperature range 1023–1223 K (1023, 1073, 1123 and 1223 K), for 3.6 up to 1080 ks, using the apparatus shown in Fig. 1.

This apparatus was equipped with a saturator, a flowmeter system, a temperature regulator and a reaction furnace. Samples suspended on a platinum wire were introduced into the reaction zone from the upper end of the quartz tube, whereas the lower end of this tube contained the zirconium solid electrolyte, ZrO_2:CaO (CSZ) sensor for monitoring the partial pressure of oxygen (p_{O_2}) in the H_2/H_2O gas mixtures. The central part of the quartz tube was heated by a resistor furnace, automatically controlled at ±2°C, the temperature being measured by means of a platinum/platinum-rhodium thermocouple (R). The moisturizing sys-

tem, called the 'saturator', consisted of a glass flask containing water, the temperature of which was adjusted to 273 K by means of a dewar filled with ice and water. The temperature of the water in the flask was checked continually with a thermometer. To obtain the H_2/H_2O vapor mixture with the composition p_{H_2}/p_{H_2O}=94/6, which is equivalent to a dewpoint of 273 K, argon containing 10% of H_2 was used as carrier gas and supplied from a cylinder. The carrier gas was passed through the saturator to absorb water vapor (p_{H_2O}=610 Pa), and was finally introduced into the reaction tube at a flow rate of 125 cm^3 min^{-1}, set by a mass flowmeter.

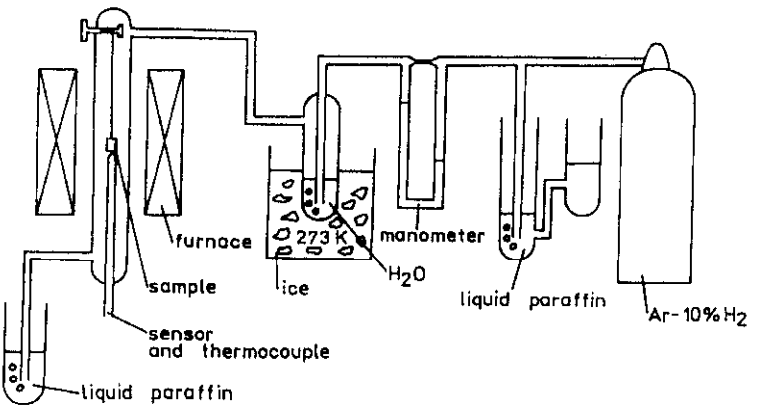

Fig. 1 Schematic diagram of the apparatus for the oxidation of alloys

The rate of oxidation of Fe–16Cr alloy was measured via the mass gains of the oxidized samples with an accuracy of 1×10^{-5} g under precisely determined thermodynamic conditions. The mass gains were used to estimate the mean thickness of the oxide films. Moreover, the thickness of the oxide film on oxidized samples in various conditions was measured separately by means of scanning electron microscopy (SEM).

The phase composition of the scale formed on the oxidized samples was identified by means of reflection X-ray diffraction, using CuK_α radiation. Microstructural characterizations of cross-sections of the samples were performed by SEM. To obtain information on the chemical compositions of the samples, the energy dispersive X-ray (EDAX) analyzer attachment of the scanning electron microscope was applied.

Results and discussion

The results of the high-temperature measurements of the oxidation kinetics for Fe–16Cr alloy under a H_2/H_2O gas mixture are presented in Figs 2 and 3. The curves of the mass gain per unit area as a function of time for the oxidation of

Fe–16Cr alloy in the H_2/H_2O gas mixture with p_{H_2}/p_{H_2O}=94/6 at various temperatures are shown in Fig. 2a, while Fig. 2b depicts the plots for the above data in the form of the mass change per unit squared as a function of time. It follows from

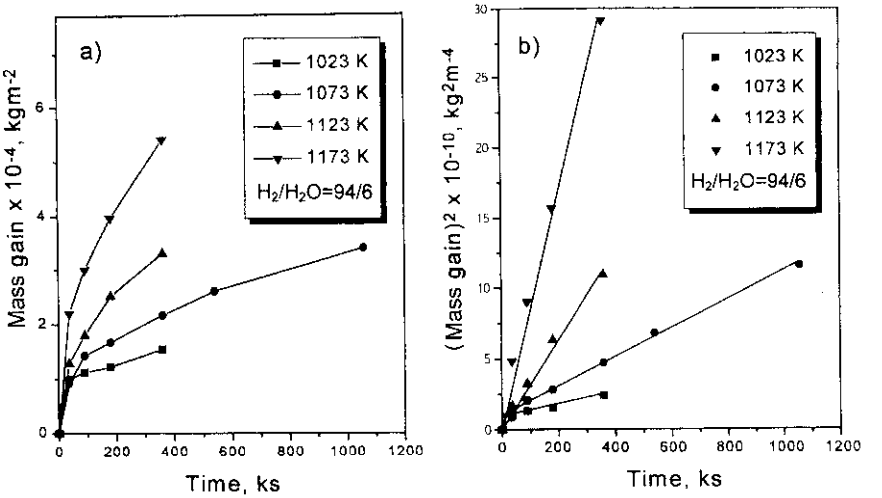

Fig. 2 a) Kinetics and b) parabolic plots expressed as mass gain per unit area for Fe–16Cr alloy oxidation in a H_2/H_2O atmosphere (p_{H_2}/p_{H_2O} = 94/6) at 1023, 1073, 1123 and 1173 K

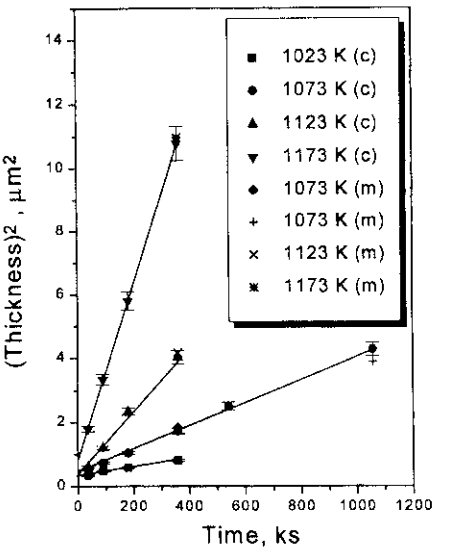

Fig. 3 Parabolic plots expressed as thickness of scale formed on Fe–16Cr alloy during oxidation in a H_2/H_2O atmosphere (p_{H_2}/p_{H_2O}= 94/6) at 1023, 1073, 1123 and 1173 K (*c* and *m* denote the calculated and the measured average thickness of the scale, respectively)

this Figure that the oxidation of the studied alloy obeys the parabolic rate law, indicating a diffusion-controlled mechanism for the times and temperatures investigated.

Figure 3 shows the curves of the scale thickness squared as a function of time for the oxidation of Fe–16Cr alloy in the H_2/H_2O gas mixture with p_{H_2}/p_{H_2O}=94/6 at various temperatures, calculated from the data presented in Fig. 2, based on Eq. (1):

$$x = \frac{\Delta m \cdot M_{MeO_v}}{16v \cdot A \cdot \rho_{MeO_v}} \tag{1}$$

where x is the thickness of layer, Δm is the mass gain of the oxidized sample, A is the surface area of the sample, ρ_{MeO_v} is the density of the scale, M_{MeO} is the molecular weight of the reaction product and 16 is the atomic weight of oxygen.

This plot also includes data concerning the thickness of the scale formed under the above-mentioned conditions, obtained by direct optical measurements using SEM.

It can be seen from Fig. 3 that the average scale thickness always corresponds to the thickness computed from the thermogravimetric data within ±7%, confirming as a consequence that the process of oxidation of Fe–16Cr alloy follows the parabolic rate law, according to the Wagner [9] equation:

$$x^2 = k_p \cdot t \tag{2}$$

where x is the thickness of the layer at time t, and k_p is the parabolic rate constant, which is a function of the self-diffusivity of the rate-determining species and the standard Gibbs energy change of the oxidation reaction.

Table 2 summarizes the experimental data, including the sample treatments, the parabolic rate constant (k_p) and the correlation coefficients (r) in regression analysis, obtained after oxidation of Fe–16Cr alloy.

Table 2 Parabolic rate constants of Fe–16Cr alloy oxidation

T/ K	Total oxidation time /ks	Atmosphere p_{H_2}/p_{H_2O}	Oxygen partial pressure/atm–	k_p/g^{2}cm^{-4}s^{-1}	r	k_p/μm^{2}s^{-1}
1023	360	94/6	$1.59 \cdot 10^{-22}$	$3.4 \cdot 10^{-14}$	0.9841	$1.2 \cdot 10^{-6}$
1073	1080	94/6	$2.35 \cdot 10^{-21}$	$8.8 \cdot 10^{-14}$	0.9817	$3.8 \cdot 10^{-6}$
1123	360	94/6	$2.76 \cdot 10^{-20}$	$2.9 \cdot 10^{-13}$	0.9968	$1.1 \cdot 10^{-5}$
1173	360	94/6	$2.62 \cdot 10^{-19}$	$7.4 \cdot 10^{-13}$	0.9973	$2.7 \cdot 10^{-5}$
1073	360	97/3	$5.2 \cdot 10^{-22}$	$7.1 \cdot 10^{-14}$	0.9927	$2.6 \cdot 10^{-6}$
1073	360	air	0.21	$8.5 \cdot 10^{-14}$	0.9859	$3.0 \cdot 10^{-6}$

It follows from a comparison of these data that the parabolic rate constant of Fe–16Cr alloy oxidation are independent of the oxygen partial pressure in the experimental range $5.2 \cdot 10^{-22}$ to 0.21 atm at a constant temperature of 1073 K. Thus, the thicknesses of the chromia scale formed on the studied alloy during the oxidation in the alloy anticipated to be exposed to both air (cathode) and H_2/H_2O gas mixture with p_{H_2}/p_{H_2O} of 94/6 or 97/3 (anode) conditions of SOFC are similar, and correspond to the calculated thicknesses of 10.5, 11.8 and 9.8 μm, respectively, after oxidation for 10 000 h under the SOFC conditions predicted an automobile.

On the basis of the k_p value (Table 2), the temperature dependence of the parabolic rate constant for oxidation of the alloy in the H_2/H_2O gas mixture with p_{H_2}/p_{H_2O}=94/6 obeys the Arrhenius equation:

$$k_p = 6.8 \cdot 10^{-4} \exp\left(-\frac{202.3 \text{ kJ mol}^{-1}}{RT}\right) \quad (3)$$

The standard error in the experimental activation energy is about ±1.3 kJ mol^{-1}.

In order to compare the experimental values of the parabolic rate constant with published values, Fig. 4 presents values of $\log k_p$ for the parabolic oxidation of Fe–Cr alloys and pure Cr as a function of the reciprocal of temperature. Moreover, Table 3 lists the activation energy (E) and pre-exponential constant (k_o) values calculated from the data in Fig. 4.

Table 3 Values of activation energies and pre-exponential constants for the oxidation of Cr and Fe–Cr alloys

Material	E/ kJ mol^{-1}	k_o/ g^2 $cm^{-4}s^{-1}$	T_{range}/ K	Ref.
Pure Cr	247	0.11	973–1473	12
Fe–20Cr	201	0.01	923–1223	10
Fe–50Cr	205	0.01	923–1273	11
Fe–16Cr	202.3	0.00068	1023–1173	present work
Cations in sintered Cr_2O_3	255	0.14 [cm^2s^{-1}]	1323–1723	13
Anions in Cr_2O_3	423	16 [cm^2s^{-1}]	1373–1723	14

It can be seen from these data that the present experimental activation energy of 202.3 kJ mol^{-1} agrees closely with the corresponding results for Fe–Cr alloys containing 20–50% Cr [10, 11] and approximately agrees with those of Hagel [12] for pure Cr oxidation at different oxygen pressures, and for cation self-diffusion in Cr_2O_3 [13], implying that the rate of oxidation for the present alloy is controlled by the outward diffusion of Cr cations in the chromia scale.

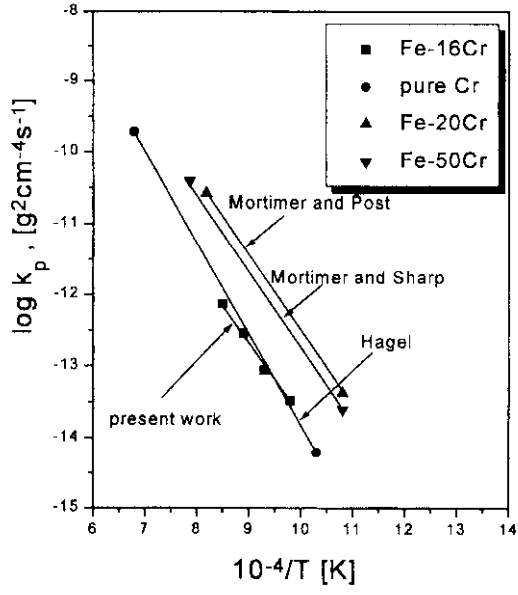

Fig. 4 Logk_p values for the parabolic oxidation of Fe–Cr alloys and pure Cr metal as functions of the reciprocal of temperature

The roentgenographic analyses have demonstrated that the structure of the oxide scales formed on Fe–16Cr alloy throughout the whole range of experimental conditions is mainly composed of Cr_2O_3. Moreover, the occurrence of the $MnCr_2O_4$ and Al_2O_3 phases, and of the α–Fe phase, originating from the substrate material, was also observed.

The morphological observations of the cross-sections of the scales formed on Fe–16Cr alloy under different thermal treatment conditions revealed that the chromia scales had uniform thickness, were compact and exhibited excellent adhesion to the metal substrate, as shown, for instance, in Fig. 5. The microchemi-

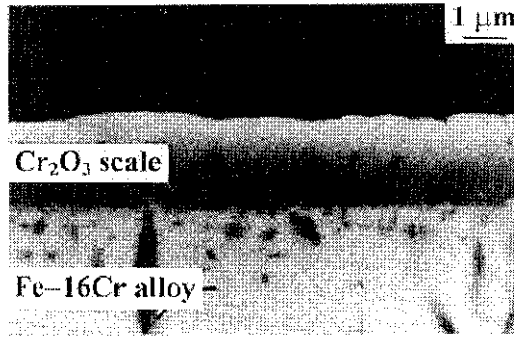

Fig. 5 SEM micrographs (BEI mode) of the cross-section of the scale formed on Fe–16Cr alloy in a H_2/H_2O gas mixture with p_{H_2}/p_{H_2O}=94/6 at 1073 K for 1058 ks

cal analysis performed by EDAX of the various parts of the oxide scale formed on Fe–16Cr alloy during the oxidation in H_2/H_2O gas mixture with p_{H_2}/p_{H_2O}=94/6 at 1073 K for 1058 ks revealed the presence of a strong concentration of Cr in the central zone of the scale, while the outer region was composed of chroma scale enriched with manganese. Moreover, this analysis also indicated that the subscale precipitates formed in the internal oxidation zone were composed of Al_2O_3. Similarly, a morphological structure was found in the case of the alloy oxidized at 1073 K for up to 360 ks in a H_2/H_2O gas mixture with p_{H_2}/p_{H_2O}=97/3 and in air.

As already mentioned, under the predicted SOFC operating conditions, a chromia scale is formed, which displays good adherence to the alloy (Fig. 5). This scale also includes a very thin non-continuous outer layer of $MnCr_2O_4$ spinel phase. The mechanism of formation of the $MnCr_2O_4$ spinel layer which is thermodynamically stable under the given experimental conditions, in spite of the very low concentration of manganese in the SUS 430 alloys (Table 1), may be explained by the faster diffusion on Mn in Cr_2O_3 than that of Cr in the oxide [15, 16]. Since the activation energies of oxidation of an alloy containing Mn and an alloy without Mn were the same and nearly corresponded to the activation energy of Cr diffusion in Cr_2O_3 it is presumed that the oxidation process of the present alloy is always accompanied by the formation of a $MnCr_2O_4$ spinel layer outside the Cr_2O_3, while the inner Cr_2O_3 oxide layer continues to grow and thicken with increasing exposure time [17].

Conclusions

1. The oxidation of Fe–16Cr (SUS 430) alloy followed a parabolic rate law throughout the whole range of temperatures (1023–1173 K) and oxygen pressures ($5.2\cdot10^{-22}$–0.21 atm), which suggests that the diffusion of ionic defects in the scale is the slowest, rate-determining step. The oxide scale was composed mainly of Cr_2O_3, with a thin $MnCr_2O_4$ spinel layer on top of the chromia scale.

2. The calculated activation energy was 202.3 kJ mol^{-1}, which is approximately the same as the values for pure Cr and Fe–Cr alloys containing 20–50% Cr.

3. The determined parabolic rate constant is independent of the oxygen partial pressure in the experimental range of $5.2\cdot10^{-22}$ to 0.21 atm at 1073 K, which means that the rates of growth of scale on Fe–16Cr alloy in air and in H_2/H_2O gas mixtures, i.e. under conditions corresponding to the operating conditions of the separator, are comparable.

4. The SUS 430 alloy containing 16% of Cr is a promising material for the separator used in the planar type of the solid oxide fuel cell.

* * *

This work was carried out as a research project of The Japan Petroleum Institute, commissioned by the Petroleum Energy Center with financial assistance from the Minsitry of International Trade and Industry. One of the authors (T. B.) is very grateful to the UNESCO and MONBUSHO of Japan for the opportunity of a one year study period as a UNESCO Fellow at the Tokyo Institute of Technology.

References

1 N. Q. Minh and T. Takahashi, Science and Technology of Ceramic Fuel Cells, Elsevier 1995.
2 T. Kadowaki, T. Shiomitsu, E. Matsuda, H. Nakagawa, H. Tsuneizumi and T. Maruyama, Solid State Ionics, 67 (1993) 65.
3 T. Shiomitsu, T. Kadowaki, T. Ogawa and T. Maruyama, Proceedings of the Fourth International Symposium on Solid Oxide Fuel Cells (SOFC-IV) (1995) 850.
4 T. Maruyama, T. Inoue and K. Nagata, Proceedings of the Fourth International Symposium on Solid Oxide Fuel Cells (SOFC-IV) (1995) 889.
5 T. Maruyama, M. Nanko, T. Brylewski and M. Tanaka, Proceedings of 26th Fall Meeting of Japan Petroleum Institute, Kyoto, Japan, November 13, 1996.
6 T. Maruyama, T. Brylewski, M. Nanko and K. Przybylski, Proceedings of Fifth International Symposium on Solid Oxide Fuel Cells, Aachen, Germany, June 2-5, 1997.
7 T. Maruyama, T. Brylewski, M. Nanko and K. Przybylski, submitted to Solid State Ionics.
8 K. Honda, T. Maruyama, T. Atake and Y. Saito, Oxidation of Metals, 38 (1992) 347.
9 C. Wagner, Z. Phys. Chem., 21 (1933) 25.
10 D. Mortimer and W. B. A. Sharp, Br. Corros. J., 3 (1968) 61.
11 D. Mortimer and M. L. Post, Corros. Sci., 8 (1968) 499.
12 W. C. Hagel, Trans. Am. Soc. Metals, 56 (1963) 583.
13 W. C. Hagel and A. W. Seybolt, J. Electrochem. Soc., 108 (1961) 1246.
14 W. C. Hagel, J. Am. Ceram. Soc., 48 (1965) 70.
15 M. G. E. Cox, B. McEnanay and V. D. Scott, Phil. Mag., 26 (1972) 839.
16 M. Shindo and T. Kondo, J. Iron Steel Inst. Japan, 68 (1982) 1628.
17 T. Tsukada, M. Shindo, T. Suzuki, H. Nakajima and T. Kondo, High Temperature Corrosion of Advanced Materials and Protective Coatings, Eds. Y. Saito, B. Önay and T. Maruyama Elsevier 1992.